University of Kurdistan
Dept. of Electrical and Computer Engineering
Smart/Micro Grid Research Center
smgrc.uok.ac.ir

Modeling of voltage source converters in microgrids using equivalent thevenin circuit

Mobin Naderi, Yousef Khayat, Qobad Shafiee, and Hassan Bevrani

Published (to be published) in: Proceedings of the 9th IEEE conference on Power Electronics, Drives Systems and Technologies, PEDSTC 2018

(Expected) publication date: 2018

Citation format for published version:

M. Naderi, Y. Khayat, Q. Shafiee, and H. Bevrani, ‘‘Modeling of voltage source converters in microgrids using equivalent thevenin circuit,’’ In Proc. 9th IEEE Power Electronics, Drives Systems, and Technologies Conference (PEDSTC 2018), Tehran, Iran, Feb. 2018, pp. 510-515.

Modeling of Voltage Source Converters in Microgrids Using Equivalent Thevenin Circuit

Mobin Naderi, Yousef Khayat, Qobad Shafiee, and Hassan Bevrani

Smart/Micro Grids Research Center, smgrc.uok.ac.ir
Department of Electrical Engineering, University of Kurdistan, Sanandaj P.C.: 6617715175, Iran
m.naderi@eng.uok.ac.ir, y.khayat@eng.uok.ac.ir, q.shafiee@uok.ac.ir, bevrani@uok.ac.ir

Abstract— **In this paper, a new modelling approach based on the equivalent Thevenin circuit is proposed for voltage source converters in islanded microgrids. The proposed method approximate the entire network connected to the voltage source converter with an equivalent Thevenin circuit. The equivalent circuit is first considered with a non-dynamic impedance. This model is simple but does not provide a good transient response. To cope with this issue, a dynamic equivalent Thevenin circuit is considered with dynamic similar to a series resistance and inductance branch. Both non-dynamic and dynamic models are validated using a microgrid test system simulated in MATLAB/SimPowerSystems.**

***Keywords*—Dynamic modeling, non-dynamic modeling, microgrids, voltage-source converter.**

I. INTRODUCTION

A basic change in the production and consumption of the electricity energy is formed in the past two decades, and it is continuing. The electricity industry has tended to the modern power grids due to some characteristics of the conventional power systems including huge losses, economic growth and electricity crisis, cost of long transmission lines and large power plants, environmental issues, and energy supply security and reliability [1]. To meet these challenges, new power grids, namely smart grids, have been proposed which intelligently monitors, predicts, and controls the behaviors of electric power users and grid operation [2]. Although the modern grids can overcome most of the conventional power system issues, they create new challenges such as high penetration of distributed energy resources (DERs). Microgrids, as a concept for integration of DERs, are good solution for the many of smart grids' challenges [3]-[5].

A microgrid is a new configuration of power systems composed of DERs and local loads, which can operate in both grid-connected and islanded modes [6]. In the islanded mode of operation, voltage and frequency regulation are the main control objectives. In fact, the stability analysis and controller design is a must important issue in the islanded microgrids [7]-[11]. To provide such an analysis and design, dynamic model of the microgrid is always required. In this regard, many dynamic models have been introduced for in the literature [12]-[15].. The existing works models all the microgrid components to design low level controllers of one DER. When this type of modeling is extended to the whole microgrid, a model with a large order may be derived [8], [13], and [15]. While, independent modeling of a DER from the rest of the microgrid results in low model order and facilitates procedure of analysis and design.

In this paper, a new modeling approach based on the equivalent Thevenin circuit is proposed for microgrids. Unlike the existing approaches, each DER is modeled independently while the rest of the microgrid components are modeled using a simple equivalent Thevenin circuit. An equivalent Thevenin circuit is considered without dynamic which ignores all dynamic effects of the rest of the microgrids on the corresponding inverter-based DER. Instead of the reminder of the microgrid, a dynamic equivalet Thevenin circuit is then studied similar to a series resistance and inductance branch. Considering such dynamic behavior improves modeling of the DER.

The rest of this paper is organized as follows. Inverter/DER modeling is fulfilled in Section II. The proposed models are verified by comparing with a simulated system in Section III. Section IV concludes the paper.

II. INVERTER MODELING

Two inverter models namely non-dynamic and dynamic models are introduced in this section. The non-dynamic model utilize a Thevenin impedance without any dynamic, while the dynamic model has a Thevenin RL branch instead of the dynamic-less impedance.

A. Non-dynamic Inverter Modeling

In this paper, the main purpose is a new modeling of *DERs* converters in islanded microgrids which are controlled as voltage sources. In this method, authors have tried to find an independent model for each DER's converter from the rest of the microgrid. In fact, based on the proposed DER model, the controller of each converter can be designed due to its local variables i.e. local voltages and currents. Therefore, the rest of the microgrid and its impact is considered as disturbance inputs and variables such as produced voltages and injected currents of all other DERs, and the impedance of all the lines and loads. Based on considering dynamics for the rest of the & the microgrid, two types of models are taken account consist of non-dynamic and dynamic. A conceptual diagram of an autonomous microgrid in a general case can show the efficiency and advantages of this modeling. This conceptual islanded microgrid diagram is shown in Fig. 1where the focus

978-1-5386-4699-1/18/$31.00 ©2018 IEEE

is on the single-line diagram of the DER_i. The DER_i is controlled as a voltage-source inverter and its DC-link voltage is assumed to be constant [16], [17]. Other DERs are operated in the form of voltage-source grid-supporting type due to islanded microgrid operation [18]. Microgrid configuration without DER_i includes other DERs, loads, and lines while they are electrically linked. The purpose is to find a model for the DER_i distinct from the rest of the microgrid. To achieve this goal, effects of the rest of the microgrid on DER_i are considered in the form of an equivalent Thevenin circuit. Fig. 2 shows the microgrid model consist of a voltage source instead of the inverter, filter inductance, capacitance, and resistances, and a Thevenin equivalent circuit. The Thevenin equivalent is composed of an impedance equivalent to all other impedances in the microgrid i.e., lines, loads, and filters, and a voltage source equivalent to all other sources in the microgrid. Three-phase equations in *abc*-frame using KVL and KCL are as follows

$$E^i_{abc} = R_i i^i_{Labc} + L_i \frac{d}{dt} i^i_{Labc} + V^i_{abc} \tag{1}$$

$$i_{Cabc_i} = i_{Labc_i} - i_{Oabc_i} = C_{f_i} \frac{d}{dt} V_{abc_i} \tag{2}$$

$$V_{abc_i} = Z_{th_i} i_{Oabc_i} + E_{th_i} \tag{3}$$

where, Z^i_{th} and E^i_{th} are calculated easily according to the structure of the rest of the microgrid. In the case of the two-DER microgrid shown in Fig. 3, Z^i_{th} and E^i_{th} are obtained as

$$\begin{cases} Z^i_{th} = Z^i_{line} + Z_{load} \parallel (Z^j_{line} + Z_j \parallel Z^j_f), \\ E^i_{th} = \left(\dfrac{(Z_j \parallel Z^j_f)(Z_{load} \parallel (Z^j_{line} + Z_j \parallel Z^j_f))}{Z_j (Z^j_{line} + Z_j \parallel Z^j_f)}\right) E^j_{an} \angle \varphi_j . \end{cases} \tag{4}$$

where, E^j_{an} is amplitude of phase voltage of the DER_j.

By replacing (3) in (1) and (2), one can write

$$E^i_{abc} = R_i i^i_{Labc} + L_i \frac{d}{dt} i^i_{Labc} + Z^i_{th} i^i_{Oabc} + E^i_{th}, \tag{5}$$

$$C^i_f Z^i_{th} \frac{d}{dt} i^i_{Oabc} = i^i_{Labc} - i^i_{Oabc}, \tag{6}$$

where two reasonable approximations are made: R_f in (2), and dE^i_{th}/dt in (6) are neglected.

Equations (5) and (6) are converted to the equivalent equations in *dq*-frame using Park and Clark transformations [19] as follows.

$$C^i_f Z^i_{th,dq} \frac{d}{dt} i^i_{Odq} + j\omega C^i_f Z^i_{th,dq} i^i_{Odq} = i^i_{Ldq} - i^i_{Odq}, \tag{7}$$

$$E^i_{dq} = R_i i^i_{Ldq} + L_i \frac{d}{dt} i^i_{Ldq} + j\omega L_i i^i_{Ldq} + Z^i_{th} i^i_{Odq} + E^i_{th,dq} \tag{8}$$

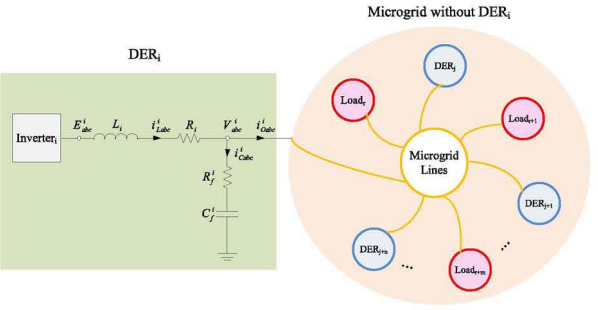

Fig. 1. General diagram of an islanded ac microgrid with focus on DER_i.

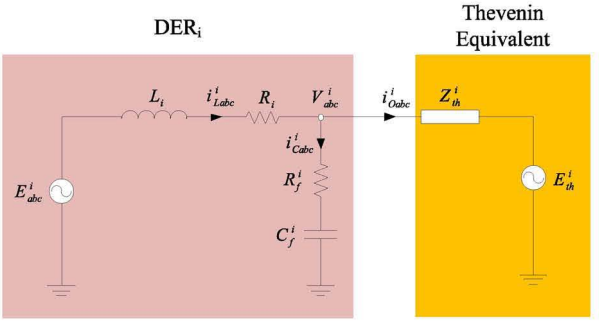

Fig. 2. The microgrid model focusing on DER_i.

where $f^i_{dq} = f^i_d + jf^i_q$ and f can be all parameters and variables including E, E_{th}, i_L, i_O, and Z_{th}. By decoupling *d* and *q* axes, (7) and (8) are expanded as

$$\begin{cases} E^i_d = R_i i^i_{Ld} + L_i \dfrac{d}{dt} i^i_{Ld} - \omega L_i i^i_{Lq} + Z^i_{th,d} i^i_{Od} - Z^i_{th,q} i^i_{Oq} + E^i_{th,d} \\ E^i_q = R_i i^i_{Lq} + L_i \dfrac{d}{dt} i^i_{Lq} + \omega L_i i^i_{Ld} + Z^i_{th,d} i^i_{Oq} + Z^i_{th,q} i^i_{Od} + E^i_{th,q} \\ i^i_{Ld} - i^i_{Od} = C^i_f Z^i_{th,d} \dfrac{d}{dt} i^i_{Od} - C^i_f Z^i_{th,q} \dfrac{d}{dt} i^i_{Oq} - \omega C^i_f Z^i_{th,q} i^i_{Od} - \omega C^i_f Z^i_{th,d} i^i_{Oq} \\ i^i_{Lq} - i^i_{Oq} = C^i_f Z^i_{th,q} \dfrac{d}{dt} i^i_{Od} + C^i_f Z^i_{th,d} \dfrac{d}{dt} i^i_{Oq} + \omega C^i_f Z^i_{th,d} i^i_{Od} - \omega C^i_f Z^i_{th,q} i^i_{Oq} \end{cases} \tag{9}$$

To derive the state space equations of the inverter model with the states $X^i = [i^i_{Ld} \quad i^i_{Lq} \quad i^i_{Od} \quad i^i_{Oq}]^T$, control inputs $U^i = [E^i_d \quad E^i_q]^T$, and disturbance inputs $W^i = [E^i_{th,d} \quad E^i_{th,q}]^T$, (9) can be rewritten as follows:

$$\begin{cases} \dfrac{d}{dt} i^i_{Ld} = -\dfrac{R_i}{L_i} i^i_{Ld} + \omega i^i_{Lq} - \dfrac{Z^i_{th,d}}{L_i} i^i_{Od} + \dfrac{Z^i_{th,q}}{L_i} i^i_{Oq} + \dfrac{1}{L_i} E^i_d - \dfrac{1}{L_i} E^i_{th,d} \\ \dfrac{d}{dt} i^i_{Lq} = -\omega i^i_{Ld} - \dfrac{R_i}{L_i} i^i_{Lq} - \dfrac{Z^i_{th,q}}{L_i} i^i_{Od} - \dfrac{Z^i_{th,d}}{L_i} i^i_{Oq} + \dfrac{1}{L_i} E^i_q - \dfrac{1}{L_i} E^i_{th,q} \\ \dfrac{d}{dt} i^i_{Od} = \dfrac{1}{K^i_{th,d}} i^i_{Ld} + \dfrac{1}{K^i_{th,q}} i^i_{Lq} - \dfrac{1}{K^i_{th,d}} i^i_{Od} + (\omega - \dfrac{1}{K^i_{th,q}}) i^i_{Oq}, \\ \dfrac{d}{dt} i^i_{Oq} = -\dfrac{1}{K^i_{th,q}} i^i_{Ld} + \dfrac{1}{K^i_{th,d}} i^i_{Lq} + (\dfrac{1}{K^i_{th,q}} - \omega) i^i_{Od} - \dfrac{1}{K^i_{th,d}} i^i_{Oq}, \end{cases} \tag{10}$$

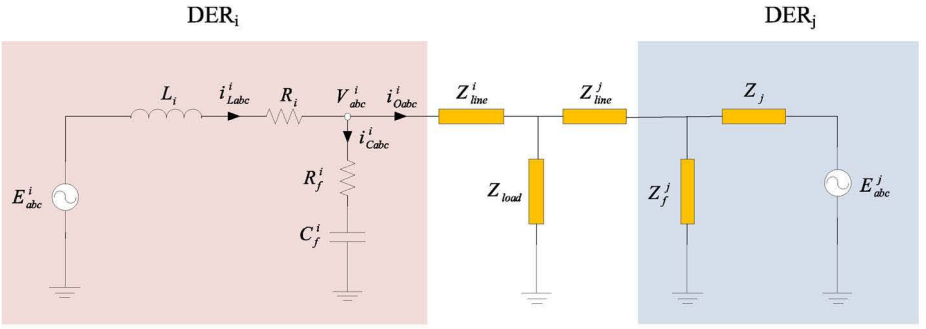

Fig. 3. A typical two-DER microgrid.

where,

$$K^i_{th,d}=\frac{C^i_f}{Z^i_{th,d}}(Z^{i\,2}_{th,d}+Z^{i\,2}_{th,q}),$$

$$K^i_{th,q}=\frac{C^i_f}{Z^i_{th,q}}(Z^{i\,2}_{th,d}+Z^{i\,2}_{th,q}).$$

Since the aim is control of the output filter voltage i.e. set of V^i_d and V^i_q, it is considered as the desired output. Thus, the differential equations (8) are expressed like a state space model.

$$\begin{cases}\dfrac{d}{dt}X^i=A^iX^i+B^i_1U^i+B^i_2W^i\\ Y^i=C^iX^i+D^i_1U^i+D^i_2W^i\end{cases}\tag{11}$$

where,

$$A^i=\begin{bmatrix}-\frac{R_i}{L_i} & \omega & -\frac{Z^i_{th,d}}{L_i} & \frac{Z^i_{th,q}}{L_i}\\ -\omega & -\frac{R_i}{L_i} & -\frac{Z^i_{th,q}}{L_i} & -\frac{Z^i_{th,d}}{L_i}\\ \frac{1}{K^i_{th,d}} & \frac{1}{K^i_{th,q}} & -\frac{1}{K^i_{th,d}} & \omega-\frac{1}{K^i_{th,q}}\\ -\frac{1}{K^i_{th,q}} & \frac{1}{K^i_{th,d}} & \frac{1}{K^i_{th,q}}-\omega & -\frac{1}{K^i_{th,d}}\end{bmatrix},$$

$$B^i_1=\begin{bmatrix}\frac{1}{L_i} & 0\\ 0 & \frac{1}{L_i}\\ 0 & 0\\ 0 & 0\end{bmatrix},\quad B^i_2=\begin{bmatrix}-\frac{1}{L_i} & 0\\ 0 & -\frac{1}{L_i}\\ 0 & 0\\ 0 & 0\end{bmatrix}.$$

To derive the output equations, (10) should be rewritten as

$$\frac{d}{dt}\begin{bmatrix}i^i_{Ldq}\\ i^i_{Odq}\end{bmatrix}=\begin{bmatrix}A^i_{11} & A^i_{12}\\ A^i_{21} & A^i_{22}\end{bmatrix}\begin{bmatrix}i^i_{Ldq}\\ i^i_{Odq}\end{bmatrix}+\begin{bmatrix}B^i_{L11} & B^i_{L12}\\ B^i_{O21} & B^i_{O22}\end{bmatrix}\begin{bmatrix}E^i_{dq}\\ E^i_{th,dq}\end{bmatrix}.\tag{12}$$

where $i^i_{Ldq}=[i^i_{Ld}\quad i^i_{Lq}]^T, i^i_{Ldq,ref}=[i^i_{Ld,ref}\quad i^i_{Lq,ref}]^T$, $i^i_{Odq}=[i^i_{Od}\quad i^i_{Oq}]^T, E^i_{dq}=[E^i_d\quad E^i_q]^T, E^i_{th,dq}=[E^i_{th,d}\quad E^i_{th,q}]^T$, and

$$A^i_{11}=\begin{bmatrix}-\frac{R_i}{L_i} & \omega\\ -\omega & -\frac{R_i}{L_i}\end{bmatrix},\quad A^i_{12}=\begin{bmatrix}-\frac{Z^i_{th,d}}{L_1} & \frac{Z^i_{th,q}}{L_1}\\ -\frac{Z^i_{th,q}}{L_1} & -\frac{Z^i_{th,d}}{L_1}\end{bmatrix},$$

$$A^i_{21}=\begin{bmatrix}\frac{1}{K^i_{th,d}} & -\frac{1}{K^i_{th,q}}\\ \frac{1}{K^i_{th,q}} & \frac{1}{K^i_{th,d}}\end{bmatrix},\quad A^i_{22}=\begin{bmatrix}-\frac{1}{K^i_{th,d}} & \omega-\frac{1}{K^i_{th,q}}\\ \frac{1}{K^i_{th,q}}-\omega & -\frac{1}{K^i_{th,d}}\end{bmatrix},$$

$$B^i_{L11}=\begin{bmatrix}\frac{1}{L_i} & 0\\ 0 & \frac{1}{L_i}\end{bmatrix},\quad B^i_{L12}=-B^i_{L11}, B^i_{O21}=B^i_{O22}=0_{2\times2},$$

Thus, one can write

$$\frac{d}{dt}i^i_{Ldq}=A^i_{11}i^i_{Ldq}+A^i_{12}i^i_{Odq}+B^i_{L11}E^i_{dq}-B^i_{L11}E^i_{th,dq}.\tag{13}$$

According to Fig. 2, the output filter voltage is calculated as

$$V^i_{dq}=E^i_{dq}+M^i_{RL}i^i_{Ldq}+M^i_L\frac{d}{dt}i^i_{Ldq},\tag{14}$$

where,

$$M^i_{RL}=\begin{bmatrix}-R_i & \omega L_i\\ -\omega L_i & -R_i\end{bmatrix},\quad M^i_L=\begin{bmatrix}-L_i & 0\\ 0 & -L_i\end{bmatrix}.$$

The derived model is called the non-dynamic model due to its non-dynamic Thevenin impedance. This model provides the stability analysis and design ability of a distinct voltage controller for any inverter in the microgrid by control effort on the output inverter voltage i.e. set of E^i_d and E^i_q. However, $E^i_{th,dq}$, the disturbance input, may affect the control procedure. Hence, disturbance attenuation may be included in the voltage controller design.

Finally, by replacing (13) in (14) the output equation of (11) is obtained with following matrices

$$C^i = \begin{bmatrix} M^i_{RL} + M^i_L A^i_{11} & M^i_L A^i_{12} \end{bmatrix},$$
$$D^i_1 = I_2 + M^i_L B^i_{L11},$$
$$D^i_2 = -M^i_L B^i_{L11}.$$

B. Dynamic Inverter Modeling

The modeling procedure is repeated while a series resistance and inductance branch is considered instead of dynamic-less equivalent Thevenin impedance of the previous subsection.

Equations (9) and (14) are rewritten as follows

$$\begin{cases} E^i_{dq} = R_i i^i_{Ldq} + L_i \dfrac{d}{dt} i^i_{Ldq} + j\omega L_i i^i_{Ldq} + Z^i_{th} i^i_{Odq} + V^i_{dq} \\ C^i_f \dfrac{d}{dt} V^i_{dq} + j\omega C^i_f V^i_{dq} = i^i_{Ldq} - i^i_{Odq} \\ V^i_{dq} = R^i_{th} i^i_{Odq} + L^i_{th} \dfrac{d}{dt} i^i_{Odq} + j\omega L^i_{th} i^i_{Odq} + E^i_{th,dq}. \end{cases} \quad (15)$$

By decoupling d and q axes, equations (15) are expanded as

$$\begin{cases} E^i_d = R_i i^i_{Ld} + L_i \dfrac{d}{dt} i^i_{Ld} - \omega L_i i^i_{Lq} + V^i_d, \\ E^i_q = R_i i^i_{Lq} + L_i \dfrac{d}{dt} i^i_{Lq} + \omega L_i i^i_{Ld} + V^i_q, \\ i^i_{Ld} - i^i_{Od} = C^i_f \dfrac{d}{dt} V^i_d - \omega C^i_f V^i_q, \\ i^i_{Lq} - i^i_{Oq} = C^i_f \dfrac{d}{dt} V^i_q + \omega C^i_f V^i_d, \\ E^i_d = R^i_{th} i^i_{Od} + L^i_{th} \dfrac{d}{dt} i^i_{Od} - \omega L^i_{th} i^i_{Oq} + E^i_{th,d}, \\ E^i_q = R^i_{th} i^i_{Oq} + L^i_{th} \dfrac{d}{dt} i^i_{Oq} + \omega L^i_{th} i^i_{Od} + E^i_{th,q}. \end{cases} \quad (16)$$

The state space equations of the inverter model with the states $X^i = [i^i_{Ld} \quad i^i_{Lq} \quad V^i_d \quad V^i_q \quad i^i_{Od} \quad i^i_{Oq}]^T$, control inputs $U^i = [E^i_d \quad E^i_q]^T$, and disturbance inputs $W^i = [E^i_{th,d} \quad E^i_{th,q}]^T$ are obtained as

$$\begin{cases} \dfrac{d}{dt} i^i_{Ld} = -\dfrac{R_i}{L_i} i^i_{Ld} + \omega i^i_{Lq} - \dfrac{1}{L_i} V^i_d + \dfrac{1}{L_i} E^i_d, \\ \dfrac{d}{dt} i^i_{Lq} = -\omega i^i_{Ld} - \dfrac{R_i}{L_i} i^i_{Lq} - \dfrac{1}{L_i} V^i_q + \dfrac{1}{L_i} E^i_q, \\ \dfrac{d}{dt} V^i_d = \dfrac{1}{C^i_f} i^i_{Ld} + \omega V^i_q - \dfrac{1}{C^i_f} i^i_{Od}, \\ \dfrac{d}{dt} V^i_q = \dfrac{1}{C^i_f} i^i_{Lq} - \omega V^i_d - \dfrac{1}{C^i_f} i^i_{Oq}, \\ \dfrac{d}{dt} i^i_{Od} = -\dfrac{R^i_{th}}{L^i_{th}} i^i_{Ld} + \omega i^i_{Oq} - \dfrac{1}{L^i_{th}} V^i_d - \dfrac{1}{L^i_{th}} E^i_{th,d}, \\ \dfrac{d}{dt} i^i_{Oq} = -\omega i^i_{Od} + \dfrac{R^i_{th}}{L^i_{th}} i^i_{Oq} + \dfrac{1}{L^i_{th}} V^i_q - \dfrac{1}{L^i_{th}} E^i_{th,q}. \end{cases} \quad (17)$$

TABLE I. MICROGRID PARAMETERS

Parameters	Value
RMS Line-Line Voltage (V)	400
Angular Frequency (rad/s)	100π
Series filter inductance ($[L_1 \quad L_2]$) (mH)	$[5 \quad 7.1]$
Series filter resistance ($[R_1 \quad R_2]$) (Ω)	$[0.3 \quad 0.3]$
Shunt filter capacitance ($[C^1_f \quad C^2_f]$) (μF)	$[20 \quad 20]$
Line impedance $[Z^1_{line} \quad Z^2_{line}]^T$ (Ω)	$\begin{bmatrix} 1.02 + j1.005 \\ 1.02 + j1.005 \end{bmatrix}$
Load impedance (Ω)	$1.898 + j0.627$
P-f droop coefficients ($[m_1 \quad m_2]$)	$[0.46 \quad 0.67] \times 10^{-4}$
Q-V droop coefficients ($[n_1 \quad n_2]$)	$[0.13 \quad 0.17] \times 10^{-2}$

The differential equations (16) are then expressed like a state space model as (11), where

$$A^i = \begin{bmatrix} -\dfrac{R_i}{L_i} & \omega & -\dfrac{1}{L_i} & 0 & 0 & 0 \\ -\omega & -\dfrac{R_i}{L_i} & 0 & -\dfrac{1}{L_i} & 0 & 0 \\ \dfrac{1}{C^i_f} & 0 & 0 & \omega & -\dfrac{1}{C^i_f} & 0 \\ 0 & \dfrac{1}{C^i_f} & -\omega & 0 & 0 & -\dfrac{1}{C^i_f} \\ 0 & 0 & \dfrac{1}{L^i_{th}} & 0 & -\dfrac{R^i_{th}}{L^i_{th}} & \omega \\ 0 & 0 & 0 & \dfrac{1}{L^i_{th}} & -\omega & -\dfrac{R^i_{th}}{L^i_{th}} \end{bmatrix},$$

$$B^i_1 = \begin{bmatrix} \dfrac{1}{L_i} & 0 \\ 0 & \dfrac{1}{L_i} \\ 0 & 0 \\ 0 & 0 \\ 0 & 0 \\ 0 & 0 \end{bmatrix}, \quad B^i_2 = \begin{bmatrix} 0 & 0 \\ 0 & 0 \\ 0 & 0 \\ 0 & 0 \\ -\dfrac{1}{L^i_{th}} & 0 \\ 0 & -\dfrac{1}{L^i_{th}} \end{bmatrix}.$$

To control the output filter voltage, output matrix is considered as

$$C^i = \begin{bmatrix} 0 & 0 & 1 & 0 & 0 & 0 \\ 0 & 0 & 0 & 1 & 0 & 0 \end{bmatrix}.$$

III. Verification of the Proposed Models

In order to verify the presented model in (9), the typical two-DER microgrid, shown in Fig. 3, with the parameters listed in Table I is simulated in the

MATLAB/SimPowerSystems. In the subsection A, the simulated inverter currents, i_{Ld}^{i} and i_{Lq}^{i}, are compared with the output of the model (9) in the presence of the most important parameters changes. The comparison between two models obtained in Section II and the simulated system is provided in the subsection B.

A. Comparison Between Non-dynamic Model and Simulated System

The non-dynamic model precision is related to the estimation of the Thevenin impedance and voltage values. These two are related to the uncertain and hard-estimated parameters consisting of the DER_j's voltage amplitude and phase i.e. E_{an}^{j}, and φ_j, respectively. The estimation error or uncertainty of each one of these parameters can mitigate the model precision. The best estimations for E_{an}^{j}, and φ_j are 408V and 18.1°, respectively according to simulated system voltage amounts, and it is considered as the basic situation. Fig. 4 shows the step responses of the simulated system and the non-dynamic model when the estimated parameters are applied. The non-dynamic model has a desired steady state response but its transient is faster than the system. Fig. 5 and Fig. 6 shows the effects of the parameters changes on the step responses of the inverter currents, i_{Ld}^{i} and i_{Lq}^{i}. In each scenario, the inverter voltage E_{an}^{i} changes from 408V to 449V at *t=0.5s* w the same input signal for the simulated system and the model, while each of the parameters changes around its nominal value as the uncertainty. Comparison between the simulated system and calculated model can be made from both steady state and transient's viewpoints.

In the steady state's point of view, the steady state error is calculated for all parameters changes, shown in Fig. 5 and Fig. 6, and is provided in Table II. According to the obtained results, it can be concluded that: 1) i_{Lq}^{i} has larger steady state error than i_{Ld}^{i}, 2) exact estimation of φ_j is harder than E_{an}^{j} but effects of φ_j on steady state error (in its range of changes around the best estimation/nominal value) is lower. 3) the steady state error of the model is acceptable for suitable estimation of the interfered uncertain parameters.

In the transient's point of view, the model step response is faster than the system step response with less settling time, and overshoot and undershoot less than 2.5 A in the best estimation. The most important reason for the difference between the model and system transients is lack of dynamics in the Thevenin impedance. In fact, dynamics of the all loads, lines and filters belong to the rest of microgrid (except DER_i), are neglected to simplify the model.

B. Comparison Between Dynamic and Non-dynamic Models and the Simulated System

Fig. 7 shows the direct and quadratic components of the DER_1's filter current. Clearly, model precision increases by considering dynamic for the equivalent Thevenin circuit. The improvement is not considerable in steady state, but in transients. Actually, both models mimic the behavior of the system in steady state, however, the dynamic model shows more accurate transient behavior. The overshoot of both

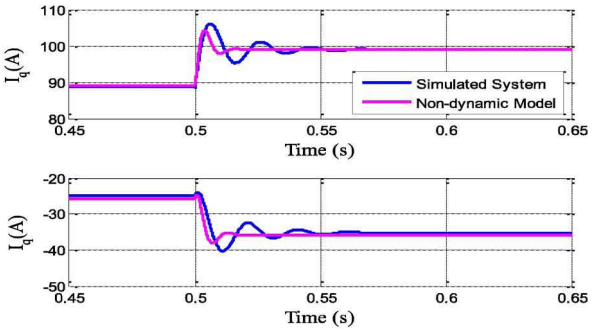

Fig. 4. Step responses of simulated system and the non-dynamic model.

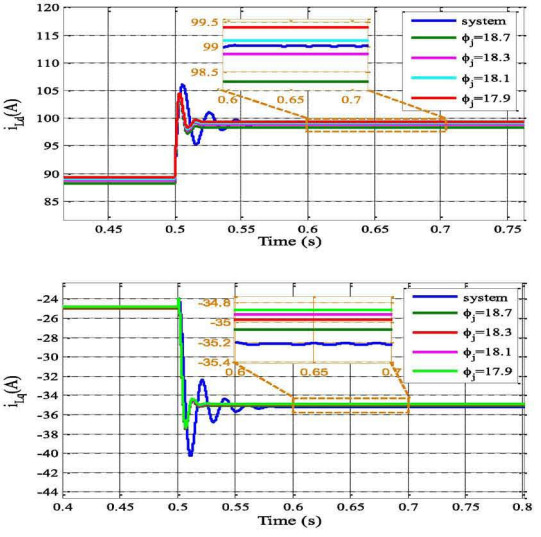

Fig. 5. Step responses of the inverter currents in the presence of DER_j voltage phase changes.

TABLE II. STEADY STATE ERROR UNDER PARAMETERS CHANGES

	φ_j (deg)				E_{an}^{j} (V)			
	17.9	18.1	18.3	18.7	390	408	418	428
i_{Ld}^{i} (%)	0.4	0.1	0.2	0.7	0.4	0.2	0.5	0.8
i_{Lq}^{i} (%)	0.9	0.8	0.7	0.4	9.1	0.6	6	11.4

models is same, almost 4 A, while it is 6 A for the simulated system. Nevertheless, the overshoot time is 0.503s, for the non-dynamic model, and 0.506s for the dynamic model and simulated system. Settling time equals to 0.52s, 0.53s, and 0.56s for the non-dynamic model, dynamic model and simulated system, respectively.

IV. CONCLUSION

This paper proposes two new state space models for voltage source converters in islanded microgrids based on equivalent Thevenin circuit; dynamic and non-dynamic models The non-dynamic model with four states can well track the setpoint with

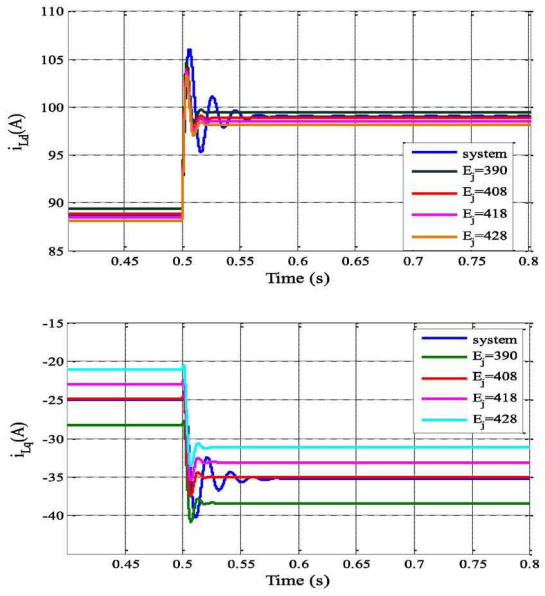

Fig. 6. Step responses of the inverter currents in the presence of DER_j voltage amplitude changes.

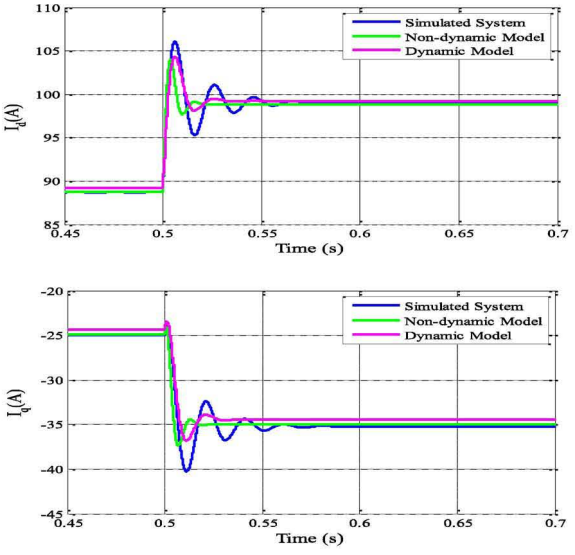

Fig. 7. Comparison of Non-dynamic model, dynamic model, and the system responses.

steady state error less than 1 %, while having faster transient. The steady state error of this model is acceptable but for suitable estimation of the interfered uncertain parameters. The dynamic model with six states provides better transient and steady state response comparing the non-dynamic model. More accurate models can be achieved by considering more desired states for the equivalent Thevenin circuit. As a future work, enhancement of the transient time will be taken in to account.

REFERENCES

[1] H. Bevrani, B. Francois, and T. Ise, Microgrid Control: Dynamics and Control, 2017.

[2] H. Bevrani, W. Masayuki, M. Yasunori, Power system monitoring and control, John Wiley & Sons, 2014.

[3] N Hatziargyriou, **H. Asano, R. Iravani, C. Marnay, "Microgrids,"** *IEEE Power Energy Mag.* vol. 5, no. 4, pp. 78-94, 2007.

[4] **R. H. Lasseter, "Microgrids,"** In Proc. *IEEE Power Eng. Soc. Winter Meeting*, , vol. 1, pp. 305-308, 2002.

[5] R. H. Lasseter, **P. Paigi, "Microgrid: A conceptual solution,"** In Proc. *35th IEEE Power Electron. Specialists Conf.(PESC 04)* vol. 6, pp. 4285-4290, 2004.

[6] W. Xiongfei, J. M. Guerrero, Z. **Chen, "Control of grid interactive AC microgrids,"** In Proc. *IEEE Int. Symp. Ind. Electron. (ISIE)*, pp. 2211-2216, 2010.

[7] J. M. Guerrero, M. Chandorkar, T. L. Lee, P.C. **Loh, "Advanced control architectures for intelligent microgrids—Part I: Decentralized and hierarchical control,"** *IEEE Trans. Ind. Electron.* vol. 60, no. 4,pp. 1254-1262, Apr. 2013.

[8] M. Y. Abdel-Rady, E. F. El-**Saadany, "Adaptive decentralized droop controller to preserve power sharing stability of paralleled inverters in distributed generation microgrids,"** *IEEE Trans. Power Electron.* vol. 23, no. 6, pp. 2806-2816, 2008.

[9] S. M. Ashabani, M. Y. Abdel-Rady, **"A flexible control strategy for grid-connected and islanded microgrids with enhanced stability using nonlinear microgrid stabilizer,"** *IEEE Trans. Smart Grid* vol. 3, no. 3, pp. 1291-1301, 2012.

[10] J. C. Vasquez, et al., **"Modeling, analysis, and design of stationary-reference-frame droop-controlled parallel three-phase voltage source inverters,"** *IEEE Trans. Industrial Electronics* vol. 60, no. 4, pp. 1271-1280, 2013.

[11] **A. P.N. Tahim, D. J. Pagano, E. Lenz, V. Stramosk, "Modeling and stability analysis of islanded DC microgrids under droop control,"** *IEEE Trans. Power Electronics* vol. 30, no. 8, pp. 4597-4607, 2015.

[12] T. Logenthiran, D. **Srinivasan, D. Wong, "Multi-agent coordination for DER in MicroGrid,"** *IEEE Int. Conf.* In *Sustain. Energy Tech.. (ICSET).* , pp. 77-82, 2008.

[13] N. Pogaku, M. Prodan**ovic, T. C. Green, "Modeling, analysis and testing of autonomous operation of an inverter-based microgrid,"** *IEEE Trans. power electronics* vol. 22, no. 2, pp. 613-625, 2007.

[14] **A, Brissette, A. Hoke, D. Maksimović, A. Pratt, "A microgrid modeling and simulation platform for system evaluation on a range of time scales,"** IEEE Conf.In *Energy Conv. Congress and Exposition (ECCE)*, , pp. 968-976, 2011.

[15] **E. Lenz, D. J. Pagano, and J. Pou, "Bifurcation analysis of parallel-connected voltage-source inverters with constant power loads,"** *IEEE Trans. Smart Grid*, no. 99, 2017.

[16] J. M. Guerrero, *et al.*, **"Wireless-control strategy for parallel operation of distributed-generation inverters,"** *IEEE Trans. Ind. Electron.*, vol. 53, no. 5, pp. 1461–1470, 2006.

[17] S. M. Ashabani, M. Y. Abdel-Rady, M. Mirsalim, M. Aghashabani. "Multivariable droop control of synchronous current converters in weak grids/microgrids with decoupled dq-axes currents." *IEEE Trans. Smart Grid* vol. 6, no. 4, pp. 1610-1620, 2015.

[18] J. Rocabert, *et al.*, **"Control of power converters in AC microgrids,"** *IEEE trans. power electron.*, vol. *27* no. 11, pp. 4734-4749, 2012.

[19] M. Naderi, *et al.*, **"Robust Multivariable Microgrid Control Synthesis and Analysis,"** *Energy Procedia* vol. 100, 375-387, 2016.